Optica Applicata, Vol. XXI, No. 1, 1991

Analytic optimization of curved holographic optical elements

A. TALATINIAN*

Institute of Physics, Technical University of Wrocław.

This paper presents a method for designing an optimal holographic optical element on a spherical substrate. The method is based on an analytic ray tracing procedure using the minimization of the mean-squared difference of the propagation vector components between the actual output wavefronts and the desired output wavefronts. The minimization yields integral equations for the grating vector components with can be solved analytical without any approximation. This procedure yields a holographic optical element that can be realized with the help of a computer-generated hologram. If the holographic lens is recorded on a curved substrate, the sine condition will be satisfied in the case when the curvature radius equals the focal length of this lens, therefore, the holographic lens removes coma aberration.

1. Introduction

Holographic optical elements (HOEs) have several advantages over conventional optical elements [1]. They are compact and lightweight. It is also simpler and cheaper to obtain large size lenses unlike conventional lenses. Generally, a hologram of a point source does not satisfy the requirements imposed by the Fourier transform lens (FTL) realization, therefore, the attempts at designing the Fourier transform lens were carried out by recording the non-spherical wavefronts which satisfy the Fourier transform requirements in an extended range of spatial frequencies. In order to minimize the aberrations, it is necessary to use the optimization procedure for designing a holographic element. Several procedures based on numerical iterative ray-techniques [2] have been proposed. The aberrations of the HOE can be corrected with the help of terms of the desired aspheric wavefronts produced by a computer generated hologram (CGH) during recording of the holographic lens. The purpose of this paper is to study FTL optimization on a spherical substrate and then to compare the results with the results of the FTL recorded on a flat substrate. There are two methods of the holographic lens optimization: one by using the grating phase function based on minimizing the mean-squared difference of the phases of the actual output and the desired output wavefronts [3]–[4], and the ray tracing method [7], [ ]. The method used here is based on analytical ray tracing

---

* On leave of absence from Institute of Physics, University of Aleppo, Syria.

that minimizes the mean-squared difference of the propagation vector components between the actual output and the desired output wavefronts. The mean-squared difference of the vector components is defined in such a way that the functions involved are continuous. Specifically, we define continuous input parameters that characterize the propagation vector components of each wavefront. Then we obtain integral equations for the optimal grating vector components which can be solved analytically without any approximation.

To illustrate our method we have designed Fourier transform lens on a spherical substrate. The performance of the lenses is analysed by ray-tracing, the results are then compared with those of quadratic HOEs and with conventional HOEs recorded on a spherical substrate by two axial symmetrical wavefronts. It is shown that under certain conditions such a holographic lens can be made aplanatic [9].

2. Optimization procedure of the HOE on a spherical substrate

A holographic optical element can be described as a complex diffraction grating which transfers the phase of an incoming wavefront to the phase of the output wavefront. The phase of the output wavefront, $\Phi_o(x,y)$, for the first diffracted order is given by

$$\Phi_o(x,y) = \Phi_i(x,y) - \Phi_h(x,y) \tag{1}$$

where $\Phi_i(x,y)$ is the phase of the input wavefront, and $\Phi_h(x,y)$ is the grating function of the HOE.

To proceed, we will now exploit the normalized propagation vectors and grating vector of the holographic element, rather than the phases of wavefronts. The normalized propagation vectors, which can be regarded as the direction cosines of the input and output rays, can be written as:

$$\hat{K}_o = \frac{\lambda}{2\pi} \operatorname{grad} \Phi_o = \frac{\lambda}{2\pi}\left(\hat{x}\frac{\partial \Phi_o}{\partial x} + \hat{y}\frac{\partial \Phi_o}{\partial y} + \hat{z}\frac{\partial \Phi_o}{\partial z}\right), \tag{2}$$

$$\hat{K}_i = \frac{\lambda}{2\pi} \operatorname{grad} \Phi_i = \frac{\lambda}{2\pi}\left(\hat{x}\frac{\partial \Phi_i}{\partial x} + \hat{y}\frac{\partial \Phi_i}{\partial y} + \hat{z}\frac{\partial \Phi_i}{\partial z}\right),$$

and the grating vector

$$\bar{K}_h = \frac{\lambda}{2\pi} \operatorname{grad} \Phi_h = \frac{\lambda}{d_x}\hat{x} + \frac{\lambda}{d_y}\hat{y} \tag{3}$$

where $\hat{x}$, $\hat{y}$, $\hat{z}$ are the Cartesian unit vectors, d_x and d_y are the grating spacing in the x and y directions, respectively, [10], and λ is the readout wavelength. For a flat HOE, defined in x-y-z coordinate system in the way that the $z = 0$ plane coincides with the surface of the HOE. The diffraction relations can be written as:

$$\hat{K}_{x_o} = \hat{K}_{x_i} \pm K_{x_h} = \hat{K}_{x_i} \pm \frac{\lambda}{2\pi}\frac{\partial \Phi_h(x,y)}{\partial x}, \tag{4}$$

$$\hat{K}_{y_o} = \hat{K}_{y_i} \pm K_{y_h} = \hat{K}_{y_i} \pm \frac{\lambda}{2\pi} \frac{\partial \Phi_h(x,y)}{\partial y}, \tag{5}$$

$$\hat{K}_{z_o} = \pm (1 - \hat{K}_{x_o}^2 - \hat{K}_{y_o}^2)^{1/2}, \tag{6}$$

with local spatial frequencies:

$$\nu_x = \frac{1}{2\pi} \frac{\partial \Phi_h(x,y)}{\partial x},$$

$$\nu_y = \frac{1}{2\pi} \frac{\partial \Phi_h(x,y)}{\partial y}.$$

If $\hat{K}_{x_o}^2 + \hat{K}_{y_o}^2 > 1$, then the output ray is evanescent and will fail to propagate away from the HOE.

The grating Equations (4)–(6) cannot be applied to the spherical substrate of the HOE. Let the direction of the incident ray at point Q of the spherical surface be inicated by $\hat{K}_i$ vector, and the grating vector that is tangent to this surface at point Q be determinated by $\vec{K}_h$. The diffracted wavefront is then defined by the direction vector $\hat{K}_o$ which is computed from Eqs. (4)–(6) used in a new coordinate system with the axis Qx' tangent to the hologram surface at point Q and the Qz' axis coincidence with the curvature radius direction at this point (see Fig. 1). The new

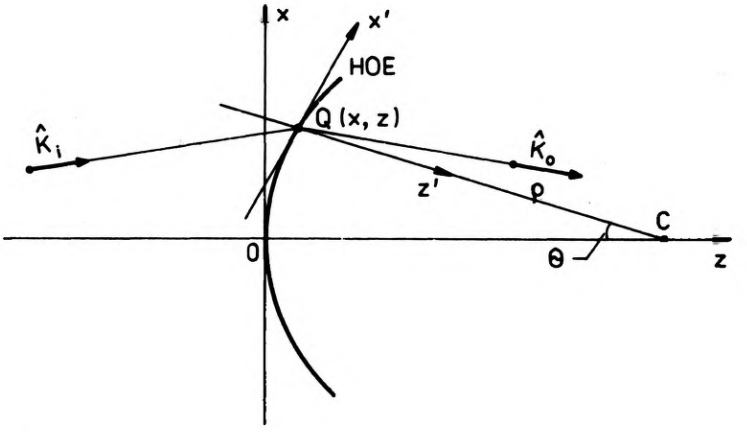

Fig. 1. Ray-tracing through a spherically curved hologram

coordinate system $Qx\,z$ is formed by rotation of the old one $0xz$ over the angle θ with regard to curvature center, where $\sin\theta = x/\rho$.

These considerations concern to the incident vector which is defined in the new coordinate system in the way

$$\hat{K}'_{x_i} = \hat{K}_{x_i} \cos\theta + \hat{K}_{z_i} \sin\theta, \tag{7}$$

$$\hat{K}'_{z_i} = -\hat{K}_{x_i} \sin\theta + \hat{K}_{z_i} \cos\theta. \tag{8}$$

Now, in the new coordinate system the Eqs. (4)–(6) take forms:

$$\hat{K}'_{x_o} = \hat{K}'_{x_i} \pm K'_{x_h} \tag{9}$$

$$\hat{K}'_{z_o} = \pm (1 - \hat{K}'^2_{x_o})^{1/2}. \tag{10}$$

At last, by transforming the $\hat{K}'_o$ vector to the old coordinate system, we obtain

$$\hat{K}_{x_o} = \hat{K}'_{x_o} \cos\theta - \hat{K}'_{z_o} \sin\theta, \tag{11}$$

$$\hat{K}_{z_o} = \hat{K}'_{x_o} \sin\theta - \hat{K}'_{z_o} \cos\theta, \tag{12}$$

where the direction vector defined in this way can be used to determine the image point coordinates in the image plane.

The goal when designing HOEs is to transfer input rays into corresponding output rays that should be optimized for a given range of input parameters. The input parameters could, for example, be the direction cosine of the incoming waves. For a single specific input parameter, it is relatively easy to form a HOE for transforming a plane wave into a spherical one. However, for a range of input parameters, it is necessary to optimize the grating vector so as to minimize the difference between the actual and the desired output rays. The optimization is achieved by minimizing the mean squared difference between these two sets of rays. To simplify the presentation of our optimization method, we will describe the method in one dimensional notation.

The mean-squared difference of the propagation vectors is defined as

$$E^2 = \iint w(a) p(x,a) [\hat{K}'_{x_d}(x,a) - \hat{K}'_{x_o}(x,a)]^2 da\, dx \tag{13}$$

where the direction cosines of the output and desired rays $\hat{K}'_{x_o}(x,a)$ and $\hat{K}'_{x_d}(x,a)$ depend on the input parameters a and x. The pupil function $p(x,a)$ can be simply a binary function: $p(x,a) = 1$ for the points x of the HOE which are illuminated by the input wavefront with parameter a, otherwise $p(x,y) = 0$. The optimization weighting function for each input parameter a is given by $w(a)$, where $0 \leqslant w(a) \leqslant 1$. Inserting Eq. (9) into Eq. (13), yields

$$E^2 = \iint w(a) p(x,a) [\hat{K}'_{x_d}(x,a) - \hat{K}'_{x_i}(x,a) + K'_{x_h}(x)]^2 da\, dx. \tag{14}$$

The optimal grating vector component $K'_{x_h}(x)$ can be determined by minimizing E^2. First, we minimize an integral which depends only on the coordinate x_o, namely

$$e^2(x_o) = \int w(a) p(x,a) [\hat{K}'_{x_d}(x_o,a) - \hat{K}'_{x_i}(x_o,a) + K'_{x_h}(x_o)]^2 da \tag{15}$$

where x_o represents an arbitrary coordinate x. Differentiating $e^2(x_o)$ with respect to $K'_{x_h}(x_o)$, and setting the result to zero, yields the optimal grating vector component

$$K'_{x_h}(x) = \frac{-\int w(a) p(x,a) [\hat{K}'_{x_d}(x,a) - \hat{K}'_{x_i}(x,a)] da}{\int w(a) p(x,a) da}. \tag{16}$$

Since the second derivative of $e^2(x_o)$ is greater than zero, the optimal grating vector yields minimum $e^2(x_o)$. For an on-axis holographic element, having circular

symmetry, the one-dimensional optimization procedure can be extended to two-dimension, the two-dimensional situation is essentially comparable to the one-dimension case after exchanging x with $r=(x^2+y^2)^{1/2}$, so the grating vector could be formed according to Eq. (16).

3. Optimal holographic Fourier-transform lens

The operation of an on-axis holographic Fourier-transform lens is described in one-dimensional representation, as shown in Fig. 2. A transparency of the input

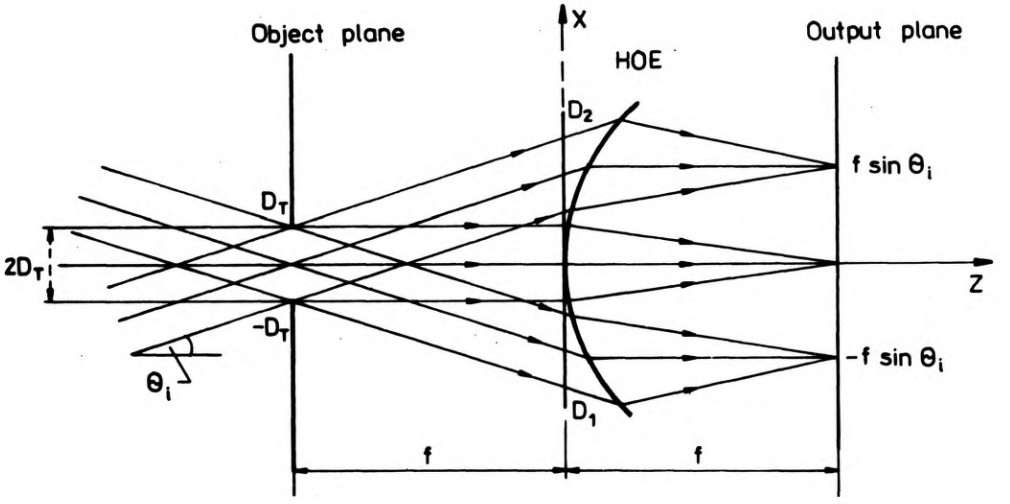

Fig. 2. Readout geometry of on-axis holographic FTL on a spherical substrate

plane is illuminated by a coherent plane wavefront. The input transparency produces an angular spectrum of plane wavefronts (one for each spatial frequency component of the input) which propagate to FTL [11]. Here, each of the input plane waves converges to a point at the output plane whose location correspnds to the angular direction of the input wave. The width of the input transparency aperture is $2D_T$, whereas the holographic lens extends from coordinate D_1 to D_2, a focal length f, which is the distance from the holographic element to the stop aperture and to the output plane. It is convenient for FTL design to let the input parameter α be a direction cosine of the plane wave emerging from the transparency, then we have

$$a=\alpha=\sin\theta_i. \tag{17}$$

Consequently, the normalized propagation vector components of the input ray is as follows:

$$\hat{K}_{x_i}(x,a)=\hat{K}_{x_i}(\alpha)=\alpha, \tag{18}$$

$$\hat{K}_{z_i}(x,a)=\hat{K}_{z_i}(\alpha)=\sqrt{1-\alpha^2}. \tag{19}$$

Now, an input plane wave having a direction cosine α must be transformed at a distance f into a spherical wave converging to a point αf. Thus, the normalized propagation vector components of the desired output rays become:

$$\hat{K}_{x_d}(x,a) = \hat{K}_{x_d}(x,\alpha) = \frac{-(x-\alpha f)}{\sqrt{(x-\alpha f)^2+(f-z)^2}}, \tag{20}$$

$$\hat{K}_{z_d}(z,a) = \hat{K}_{z_d}(z,\alpha) = \frac{f-z}{\sqrt{(x-\alpha f)^2+(f-z)^2}} \tag{21}$$

where z_Q is a function of x determinated by the hologram shape

$$z_Q = |\rho| - \sqrt{\rho^2 - x^2}. \tag{22}$$

ρ is the curvature radius of the spherical holographic lens substrate. Substituting $\hat{K}_{x_i}$, $\hat{K}_{z_i}$ from Eqs. (18), (19) and $\hat{K}_{x_d}$, $\hat{K}_{z_d}$ from Eqs. (20), (21) into Eq. (16) and by using Eq. (7) for the desired vector output rays, we have

$$\hat{K}'_{x_d} = \hat{K}_{x_d}\cos\theta + \hat{K}_{z_d}\sin\theta, \tag{23}$$

and for $w(\alpha) = 1$, we obtain

$$K'_{x_h}(x) = -\frac{1}{\alpha_2(x)-\alpha_1(x)} \int_{\alpha_1(x)}^{\alpha_2(x)} \left[\frac{x}{\rho} \frac{(f-z)}{\sqrt{(x-\alpha f)^2+(f-z)^2}} - \sqrt{1-\left(\frac{x}{\rho}\right)^2} \frac{(x-\alpha f)}{\sqrt{(x-\alpha f)^2+(f-z)^2}} - \frac{x}{\rho}\sqrt{1-\alpha^2} - \sqrt{1-\left(\frac{x}{\rho}\right)^2}\alpha \right] d\alpha \tag{24}$$

where the pupil function $p(x,a)$ is expressed by the upper $\alpha_2(x)$ and lower $\alpha_1(x)$ direction cosines of the input plane waves which intercept the spherical substrate holographic lens at a point x.

The solution of Equation (24) is given by

$$\begin{aligned} K'_{x_h}(x) = \frac{-1}{[\alpha_2(x)-\alpha_1(x)]} \Bigg\{ & -\frac{x}{\rho}\left(\frac{f-z}{f}\right) \\ & \times \ln\left| \frac{(x-\alpha_2(x)f)+\sqrt{(x-\alpha_2(x)f)^2+(f-z)^2}}{(x-\alpha_1(x)f)+\sqrt{(x-\alpha_1(x)f)^2+(f-z)^2}} \right| \\ & + \sqrt{1-\left(\frac{x}{\rho}\right)^2}\frac{1}{f}\left[\sqrt{(x-\alpha_2(x)f)^2+(f-z)^2} - \sqrt{(x-\alpha_1(x)f)^2+(f-z)^2}\right] \\ & - \frac{1}{2}\frac{x}{\rho}\left[\arcsin\alpha_2(x) + \alpha_2(x)\sqrt{1-\alpha_2^2(x)}\right. \\ & \left. - \arcsin\alpha_1(x) - \alpha_1(x)\sqrt{1-\alpha_1^2(x)}\right] - \frac{1}{2}\sqrt{1-\left(\frac{x}{\rho}\right)^2}\left[(\alpha_2(x)-\alpha_1(x))\right. \\ & \left.(\alpha_2(x)+\alpha_1(x))\right]\Bigg\}. \end{aligned} \tag{25}$$

We see that the grating vector for a flat holographic lens can be obtained as a limit curvature radius which approaches to infinity. Then we have [8]

$$\lim_{\rho\to\infty}\left[K'_{x_h}(x)\right]_{opt} = \left[K_{x_h}(x)\right]_{opt} = \frac{\alpha_1(x)+\alpha_2(x)}{2} - \frac{1}{\alpha_2(x)x-a_1(x)}\frac{1}{f}\left[\sqrt{(x-a_2(x)f)^2+f^2}-\sqrt{(x-\alpha_1(x)f)^2+f^2}\right], \tag{26}$$

the lower direction cosine $\alpha_1(x)$ is given by

$$\alpha_1(x) = \frac{x+D_T}{\sqrt{(x+D_T)^2+(f+z)^2}}, \tag{27}$$

ant the upper direction cosine

$$\alpha_2(x) = \frac{x-D_T}{\sqrt{(x-D_T)^2+(f+z)^2}}, \tag{28}$$

The solution given by Equation (25) is rather general and can be simplified by approximating to optimal designs. For example, it is possible to expand Eq. (25) by assuming the paraxial approximation for large f/x and also for large ρ/x. For rotationally symmetrical curved holograms the point Q can be considered to lie on the best fitting sphere at the vertex. This makes the theory especially suitable for holograms of small diameter and we have

$$z_Q \approx |\rho| - (\rho^2-x^2)^{1/2} \approx \frac{1}{2}\frac{x^2}{\rho} - \frac{1}{8}\frac{x^4}{\rho^3} + \ldots, \tag{29}$$

the approximate solution for the quadratic on-axis FTL given by a 3rd order Tailor expansion. This leads to a simpler holographic grating vector

$$\left[K'_{x_h}(x)\right]_{simplifield} \approx \frac{x}{f} = \left[K'_{x_h}(x)\right]_q. \tag{30}$$

For comparison, we performed a ray tracing analysis for an on-axis Fourier transform holographic lens recorded by two axial symmetrical wavefronts. It can be shown that such a Fresnel zone hologram, shown in Fig. 3, can satisfy the requirements of an FTL covering an extended band of spatial frequencies [12], [13].

Now, the object and reference beams with the direction cosines defined by Eqs. (4)–(6) interfere during the recording process. The resulting exposure of the fringes distribution is proportial to the term

$$\cos\left(K_{x_h}(x)+K_{y_h}(y)+K_{z_h}(z)\right). \tag{31}$$

Therefore the grating vector can be written in the form

$$K_h(x,y) = K_{O1}(x,y) - K_R(x,y) = \nabla\Phi_q(x,y) \tag{32}$$

where $q = (O_1, R)$ the indices of the object and reference waves, respectively, and ∇ is

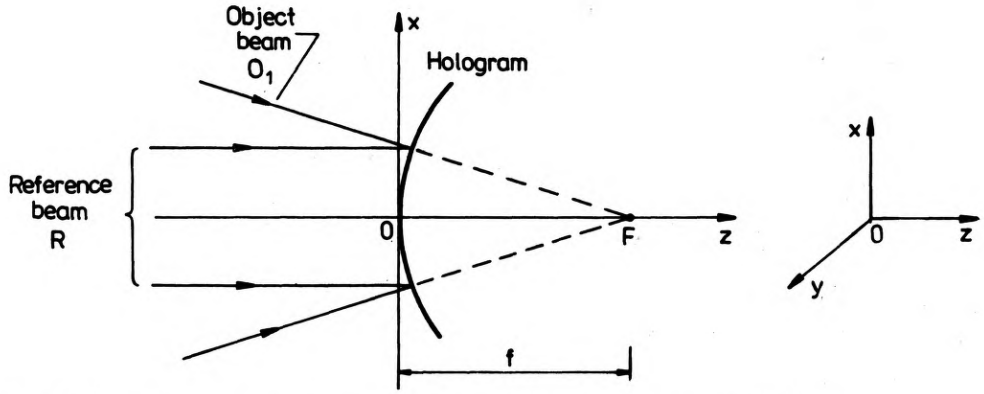

Fig. 3. Recording geometry of the axial symmetrical HOE on a spherical substrate

the gradient operator. The normalized propagation vector components of the object and reference rays are given by

$$K_{O_1} = \left(\frac{-x}{\sqrt{x^2+y^2+(f-z)^2}}, \frac{-y}{\sqrt{x^2+y^2+(f-z)^2}}, \frac{f-z}{\sqrt{x^2+y^2+(f-z)^2}} \right), \tag{33}$$

$$K_R = (0,0,1). \tag{34}$$

The HOE spherical grating vector is then given by

$$K'_{x_h}(x) = \frac{x}{\rho} \frac{(f-z)}{\sqrt{x^2+(f-z)^2}} - \sqrt{1-\left(\frac{x}{\rho}\right)^2} \frac{x}{\sqrt{x^2+(f-z)^2}} - \frac{x}{\rho}. \tag{35}$$

As an illustration, we chose specific values of the parameters: $f = 60$ mm, $2D_T = 20$ mm, $D_2 = -D_1 = 25$ mm, $\rho = (\infty, 200, 600)$ mm, and the angular range of the input plane waves for $\theta_{max} = -\theta_{min} = 14°$, we evaluated the performance of the optimal FTL by using a ray tracing analysis. For comparison, we also performed a ray tracing analysis for a quadratic FTL as well as for a spherical FTL. The spot size as a function of the input angles for the optimal, the quadratic, and spherical FTLs is shown in Fig. 4, where the results do not take into account the diffraction effects from the aperature. The spot size was determined by calculating the standard deviation of the location of the rays at the output plane as a function of the angular directions for each input plane wave. Figure 4**a** shows the spot size for the spherical FTL on a spherical substrate which is better then for a flat FTL.

Figures 4**b** and 4**c** illustrate the spot size for the optimal and quadratic FTLs produced on a spherical substrate which are better than for the spherical FTL. By subtracting the actual (average) location of each spot from the desired location the amount of distortion was calculated. The desired focussing location of the input plane wave at θ_{x_i} is αf. Figure 5 shows the distortion as a function of the input angle θ_{x_i}, for $\rho = 600$ mm, and $f = 60$ mm, and $2D_T = 20$ mm. The distortions for the quadratic and optimal element are significantly smaller than those for the spherical element.

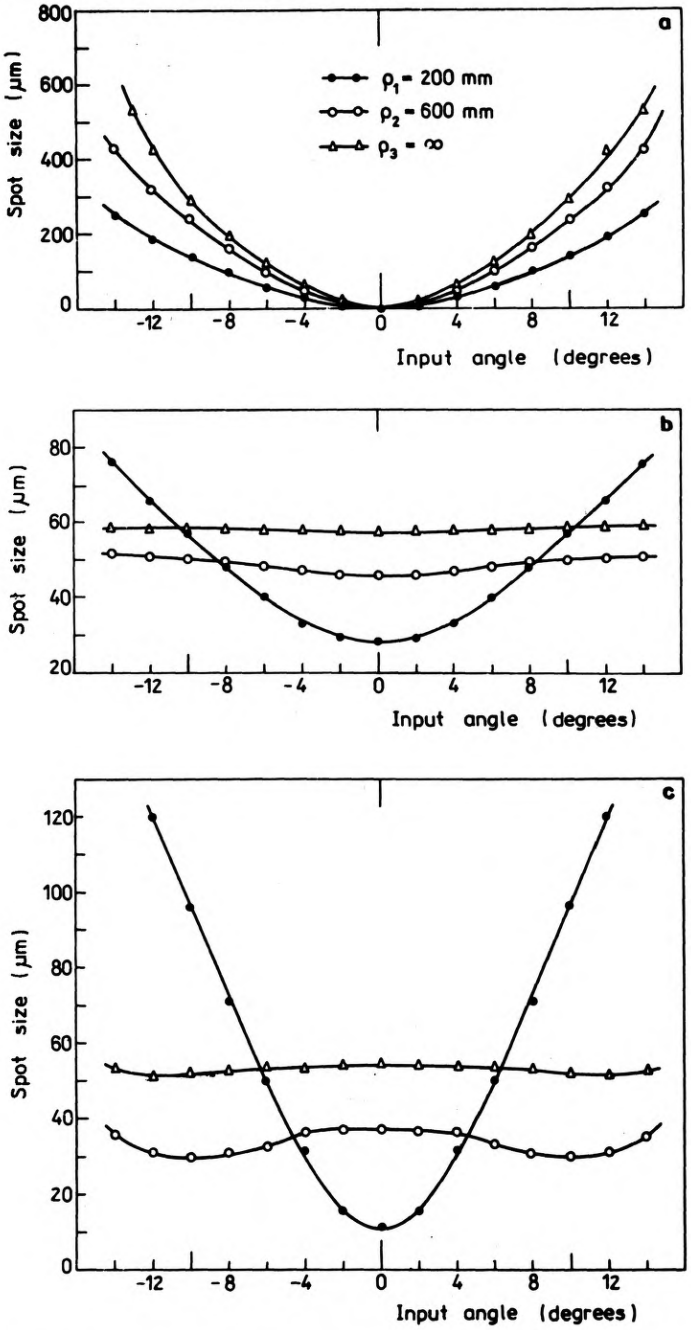

Fig. 4. Spot size as a function of the input angle for an on-axis FTL, for three different values of curvature radius ρ. Spherical grating vector – **a**, quadratic grating vector – **b**, optimal grating vector – **c**

Figure 6 shows a comparison between a holographic spherical FTL recorded on a flat substrate and the holographic lens on a spherical substrate. The focal length was $f = 100$ mm, and $2D_T = 10$ mm, and the curvature radius of the lens $\rho = (\infty,$

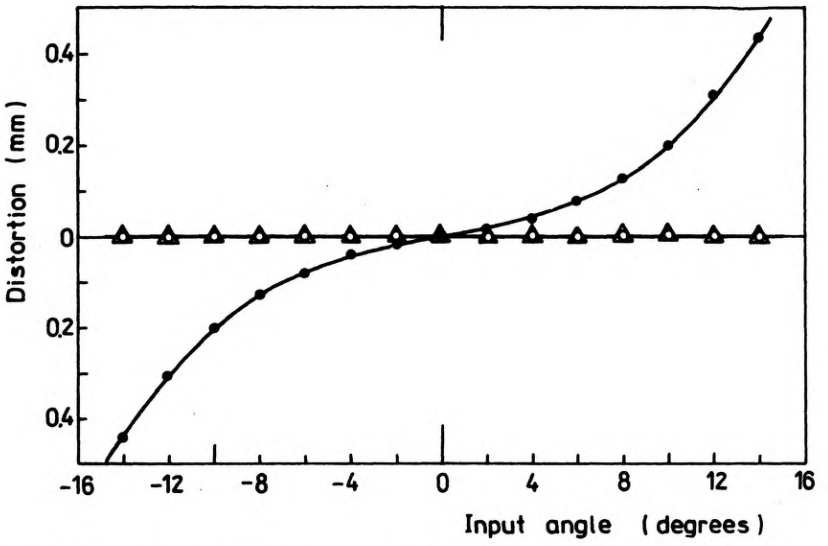

Fig. 5. Distortion as a function of input angle θ_i, for spherical (•), quadratic (△), and optimal (o) grating vectors

100, 200) mm. The spot diagrams were calculated for nine different input plane waves with $-5°$, $0°$, and $5°$ in both x and y directions. Figures 6**a** and **b** show the small central spot diagram for the spherical lenses, because the recording and readout geometries are in this case identical. However, as the readout input angles differ from the recording angles, the spot diagrams spread substantially. Here, the spot diagrams for spherical lens on a spherical substrate is better than for a lens recorded on a flat substrate.

In Figure 6**c** we see the spot diagrams for $\rho = f = 100$ mm, and the sine condition is satisfied, beacuse of the relation $x = f \sin\theta_i$. In this case coma aberration is removed, beacuse the centre of the spherical hologram substrate is brought into agreement with the focal point, and the curvature radius is equal to the focal length of this holographic lens, and the spherical aberration compensated for $\mu = 1$ (it is the ratio between the readout and recording wavelengths). We say that the holographic spherical lens is aplanatic.

Figure 7 shows a comparison spot diagrams for the three lenses, the results for $f = 60$ mm, $2D_T = 10$ mm, and $\rho = 600$ mm. In Fig. 7**a** we see the spot diagrams for the spherical lens for three input plane waves sloped at $0°$, $5°$ and $10°$, whereas in Figs. 7**b** and 7**c** spot diagrams for the quadratic and the optimal lenses are shown respectively. As shown in Fig. 7**a** the small central spot diagram for the spherical FTL is essentialy ideal because the recording and readout geometries are identical. Whereas in quadratic FTL in Fig. 7**b** and optimal FTL in Fig. 7**c**, the central spot diagram is larger. However, as the readout angles increase, the spread in the spot diagrams is much smaller than for the spherical FTL.

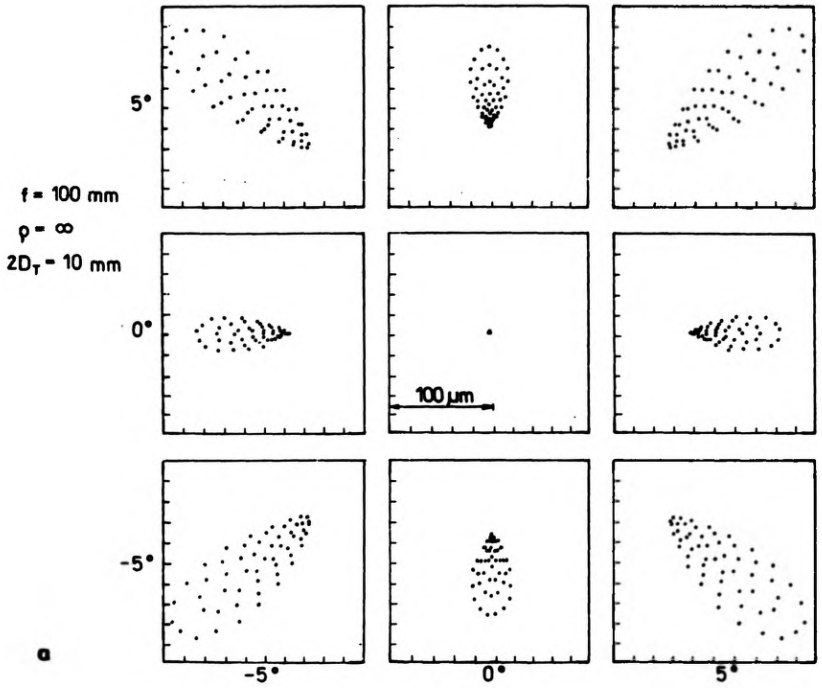
f = 100 mm
ρ = ∞
2D_T = 10 mm
5°
0°
-5°
100 µm
-5°
0°
5°
a

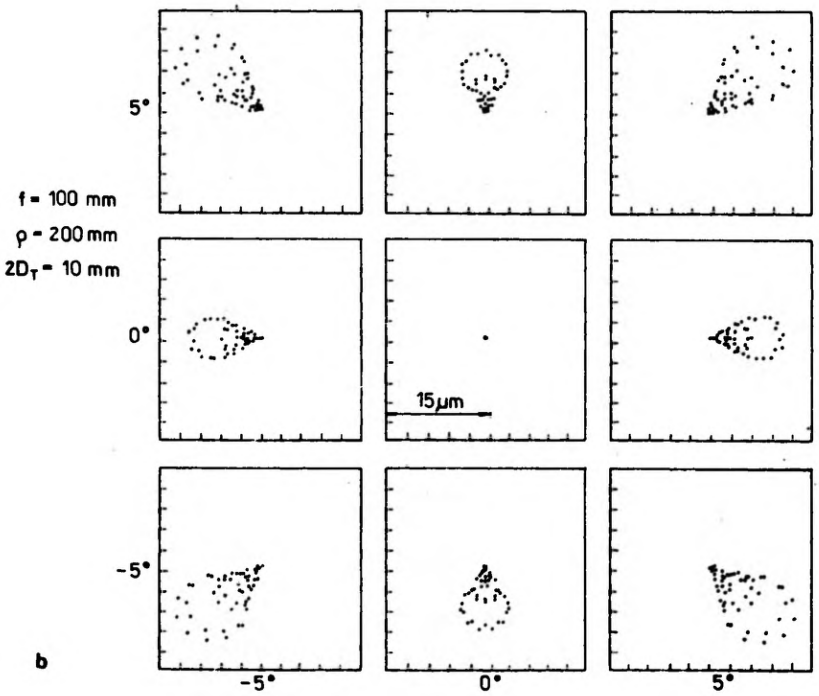
f = 100 mm
ρ = 200 mm
2D_T = 10 mm
5°
0°
-5°
15 µm
-5°
0°
5°
b

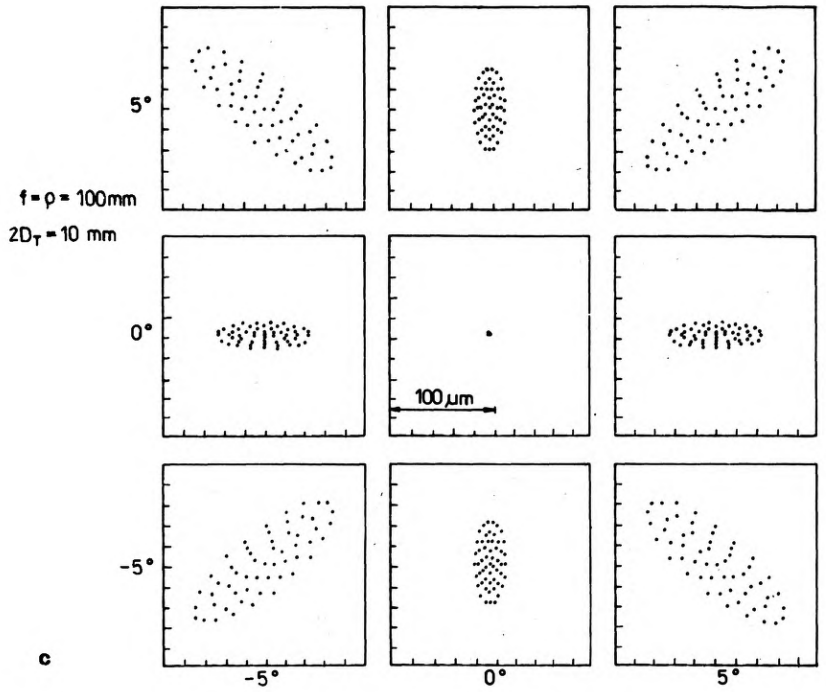

Fig. 6. Spot diagrams for the on-axis FTL: **a** – spherical grating vector on a flat substrate, **b** – spherical grating vector on a spherical substrate, **c** – spherical grating vector on a spherical substrate

4. Conclusions

In this paper, we have studied the problem of designing an optimal holographic optical element on a spherical substrate. It is necessary to optimize the grating vector, i.e., to minimize the difference between the actual output and the desired output wavefronts. Our optimization method is based on analytic ray tracing, which provides an analytic solution for the optimal grating vector without any approximation.

The necessary arbitrary grating function can be realized by resorting to the computer-generated hologram.

For the holographic FTL which is recorded on a spherical substrate, the sine condition is satisfied to remove coma and spherical aberration. Such a holographic FTLs is an aplanatic lens. The results are illustrated by the spot size as a function of the input angles for the optimal, the quadratic and the spherical FTLs. By bending the flat substrate of holographic lens the image was improved, and angular range of spatial frequencies enlarged. The results revealed that lenses designed with the presented optimization method are better when formed on the spherical substrate than on a flat substrate, and can be applicable succesfully in holographic Fourier transformation.

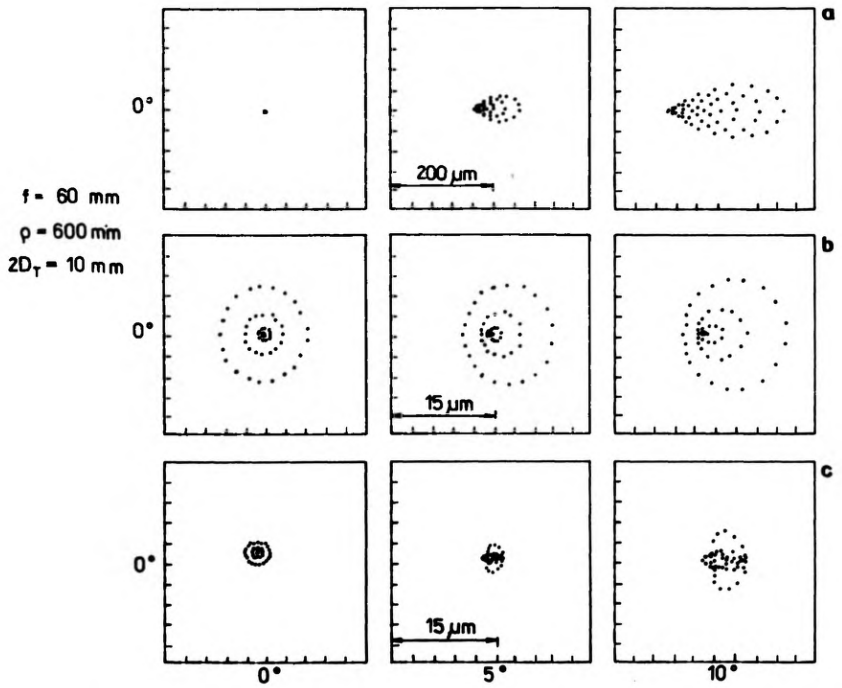

Fig. 7. Spot diagrams for the on-axis FTL: **a** – spherical grating vector, **b** – quadratic grating vector, **c** – optimal grating vector

Acknowledgements – This work has been sponsored by the CPBP 01.06 Research Program, and was presented at IX Czechoslovak-Polish Optics Conference in Hradec and Moravici in September 25–29, 1990. The author wishes to express his thanks to Prof. E. Jagoszewski and Dr M. Pluta for inspiration and many helpful discussions.

References

[1] CLOSE D. H., Opt. Eng. **14** (1975), 408.
[2] FARCHILD R. C., FIENUP J. R., Opt. Eng. **21** (1982), 133.
[3] WINICK K. A., FIENUP J. R., J. Opt. Soc. Am. **73** (1983), 208.
[4] KEDMI J., FRIESEM A. A., J. Opt. Soc. Am. A **3** (1986), 2011.
[5] CEDERQUIST J. N., FIENUP J. R., J. Opt. Soc. Am. A **4** (1987), 699.
[6] KEDMI J., FRIESEM A. A., Appl. Opt. **23** (1984), 4015.
[7] HASMAN E., DAVISON N., FRIESEM A. A., Rev. Roum. Phys. **33** (1988), 643.
[8] HASMAN E., FRIESEM A. A., J. Opt. Soc. Am. A **6** (1989).
[9] WELFORD W. T., J. Phot. Sci. **23** (1975), 84.
[10] LATTA J. N., Appl. Opt. **10** (1971), 2698.
[11] GOODMAN J. W., *Introducing to Fourier Optics*, Mc Graw-Hill Co., New York 1968, pp. 77–96.
[12] JAGOSZEWSKI E., Optik **83** (1989), 151.
[13] JAGOSZEWSKI E., Optik **69** (1985), 85.

Received November 25, 1990
in revised form December 14, 1990

Аналитическая оптимизация голографических оптических элементов на искривленных основаниях

Представлен метод конструкции оптимальных оптических элементов на сферическом основании. Метод базирует на процедуре аналитической передачи хода лучей при применении минимизации разности средней квадратичной составляющих вектора распространения между актуальными и желаемыми выходными волновыми фронтами. Минимизация дает интегральное уравнение для составляющих вектора решетки, которые можно решить аналитически без какого-нибудь приближения. Эта процедура определяет голорафический оптический элемент, который можно реализовать в виде синтетических голограмм. Если голографическая линза зарегистрирована на искривленном основании, условиям синусов будет удовлетворено в случае, когда радиус кривизны равен фокусному расстоянию этой линзы и в результате будет устранена концентрическая аберрация.

Перевел Станислав Ганцаж